ISBN: 978-3-95450-227-1 ISSN: 2673-5490 doi:10.18429/JACoW-IPAC2022-TUPOPT023

UNDULATOR TAPERING STUDIES OF AN ECHO-ENABLED HARMONIC GENERATION BASED FREE-ELECTRON LASER

F. Pannek*, W. Hillert, University of Hamburg, Hamburg, Germany
S. Ackermann, E. Ferrari, L. Schaper, Deutsches Elektronen-Synchrotron DESY, Hamburg, Germany

Abstract

The free-electron laser (FEL) user facility FLASH at DESY is currently undergoing an upgrade which involves the transformation of one of its beamlines to allow for external seeding via so-called Echo-Enabled Harmonic Generation (EEHG). With this seeding technique it will be possible to provide stable, longitudinal coherent and intense radiation in the XUV and soft X-ray regime at high repetition rate. To ensure an efficient FEL amplification process, sustainable energy exchange between the electrons and the electromagnetic field in the undulator is mandatory. Adequate adjustment of the undulator strength along the beamline allows to compensate for electron energy loss and to preserve the resonance condition. The impact of this undulator tapering on the temporal and spectral characteristics of the EEHG FEL radiation at 4 nm is investigated by means of numerical simulations performed with the FEL code GENESIS1.3, version 4. Different tapering methods are examined and it is shown that specific tapering of the undulator strength allows to exceed the FEL saturation power while maintaining a clear temporal and spectral shape of the FEL pulse.

INTRODUCTION

In the Echo-Enabled Harmonic Generation (EEHG) seeding scheme [1] density modulations at high harmonics of the seed laser wavelength are imprinted on an electron bunch before it is injected into a subsequent undulator radiator for free-electron laser (FEL) emission. Due to the pre-bunched electron beam the amplification in the radiator develops fast. A long radiator section makes it crucial to adjust the undulator strength of the individual radiator modules along the beamline to exceed the saturation power of the FEL [2, 3].

In the following, different undulator tapering methods and their effect on the spectro-temporal characteristics of the FEL radiation are studied for an EEHG based FEL at 4 nm. For this, numerical simulations with the FEL code GENESIS1.3, v4 [4, 5] are carried out within the parameter range of the future FLASH2020+ upgrade [6] of the FEL user facility FLASH at DESY [7–9].

EEHG SETUP

The longitudinal phase space distribution of the electron bunch is manipulated in two undulators, so-called modulators, where the electrons interact with a seed laser and are modulated in energy. The resulting energy modulation amplitudes A_1 and A_2 are expressed as a multiple of the rms beam energy spread σ_E. Each modulator is followed by a chicane to create longitudinal dispersion $R_{56,1}$ and $R_{56,2}$. Parameters used in the simulations are listed in Table 1. The current distribution as well as the power profiles of the two seed lasers are Gaussian, where τ is the full width at half maximum. Proper adjustment of the EEHG setup results in a peak bunching of about 5 % at the entrance of the radiator, as shown in Fig. 1. Note that the energy spread in the area with high bunching increases up to 635 keV.

Table 1: Simulation Parameters for EEHG at 4 nm

Electron Beam		Seed Lasers		EEHG	
E	1.35 GeV	λ_1	300 nm	A_1	5
σ_E	150 keV	λ_2	300 nm	A_2	3
I_p	500 A	τ_1	150 fs	$R_{56,1}$	7.05 mm
ε_n	0.6 mm mrad	τ_2	50 fs	$R_{56,2}$	81.25 µm
τ_e	314 fs				

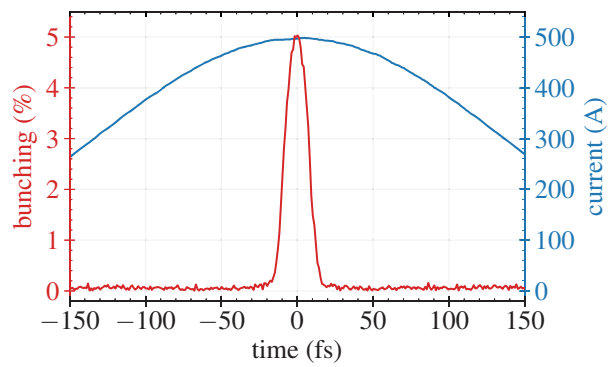

Figure 1: Bunching at 4 nm and current profile (calculated within 300 nm slices) before entering the radiator.

UNDULATOR TAPERING

The radiator beamline is made up of 11 helical undulator modules of $L_\mathrm{u} = 2.508$ m length with a $\lambda_\mathrm{u} = 33$ mm period length. Quadrupoles located between the modules are used for proper matching, resulting in an average rms transverse electron beam size of $\sigma_{x,y} = 45.5$ µm along the radiator. The undulator strength $K = K_\mathrm{rms}$ is set to a constant value along each individual module. The undulator strength K_r derived from the FEL resonant condition for a resonant wavelength of $\lambda_\mathrm{r} = 4$ nm serves as reference:

$$\lambda_\mathrm{r} = \frac{\lambda_\mathrm{u}}{2\gamma_\mathrm{r}^2}\left(1 + K_\mathrm{r}^2\right), \tag{1}$$

where the initial electron energy is given by the Lorentz factor γ_r.

* fabian.pannek@desy.de

ISBN: 978-3-95450-227-1 ISSN: 2673-5490 doi:10.18429/JACoW-IPAC2022-TUPOPT023

Time-dependent simulations have shown that the pulse energy of the FEL radiation is maximized after the first radiator module when the K value is detuned by $\Delta K = -0.1\,\%$ with respect to K_r. However, simulations have also shown that, after tapering, an initial detuning by $\Delta K = -0.05\,\%$ results in slightly higher final peak power at the end of the beamline. Note that the influence of the first few radiators on the spectral properties is rather negligible after tapering, but to start from a common basis, all radiators are initially detuned by this value.

In the following, different methods are utilized to find optimum undulator strengths: linear tapering, quadratic-linear tapering and iterative tapering. For each method, the K values of the radiator modules are scanned for maximum radiation power at the end of the beamline. The optimization is based on steady-state simulations, which do not consider time-dependent effects such as slippage. Figure 2 shows the corresponding optimum sets of K values.

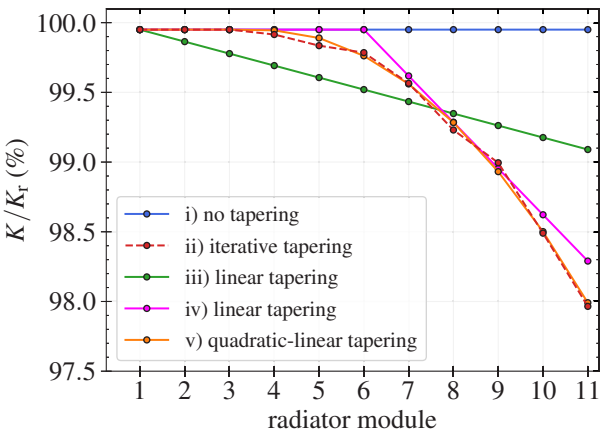

Figure 2: Different methods of undulator tapering.

Iterative Tapering

Radiator modules 1–3 are fixed to the same initial K value and not varied during the optimization procedure. Modules 4–11 are initially opened, that is, the undulator strength is set to zero. Starting with the fourth radiator module, each radiator module is scanned for maximum radiation power at the end of the beamline and set to the respective optimum K, before proceeding with the next module. After optimizing the last module, the process is repeated in reverse order for several iterations until convergence is achieved within the desired accuracy (dashed red curve in Fig. 2).

Linear Tapering

The undulator strength is decreased linearly along the radiator modules. The linear dependency results in a tradeoff between small detuning at the initial stage of the beamline and large detuning at the end, where the electrons lose more energy (green curve in Fig. 2). The radiation power can be maximized when starting the linear tapering after six modules (magenta curve in Fig. 2).

Quadratic-Linear Tapering

The optimum undulator strength can be calculated by the detuning parameter C:

$$K = \sqrt{\lambda_\mathrm{r}\gamma_0^2\left(\frac{2}{\lambda_\mathrm{u}} - \frac{C}{\pi}\right) - 1}\,. \tag{2}$$

Following the general law of undulator tapering presented in [3], the detuning along the undulator distance z_u can be fitted by two coefficients α_tap and β_tap and the start position z_0 of the tapering:

$$\hat{C} = \alpha_\mathrm{tap}(\hat{z}_\mathrm{u} - \hat{z}_0)\left[\arctan\left(\frac{1}{2N}\right) + N\ln\left(\frac{4N^2}{4N^2+1}\right)\right], \tag{3}$$

where the Fresnel number N is given by $N = \beta_\mathrm{tab}/(\hat{z}_\mathrm{u} - \hat{z}_0)$. $C = \Gamma\hat{C}$ and $z_\mathrm{u} = \Gamma/\hat{z}_\mathrm{u}$ are scaled with the gain parameter

$$\Gamma = \left[\frac{I}{I_\mathrm{A}}\frac{8\pi^2 K_0^2}{\lambda_\mathrm{r}\lambda_\mathrm{u}\gamma_0^3}\right]^{1/2}. \tag{4}$$

Here, $I_\mathrm{A} \approx 17\,\mathrm{kA}$ is the Alfvén current and the beam current I is set to the peak value I_p of the current distribution. The parameter $\beta_\mathrm{tap} = 8.5 \cdot B$ is approximated by the diffraction parameter

$$B = 2\Gamma\sigma_{x,y}^2\frac{2\pi}{\lambda_\mathrm{r}}\,. \tag{5}$$

Since this approach provides a continuously changing $K(z_\mathrm{u})$ along an infinitely long undulator, the arithmetic mean value of $K(z_\mathrm{u})$ is calculated within distances of L_u and used for the corresponding radiator module in the FEL beamline. To account for the initial detuning of $\Delta K = -0.05\,\%$, K_0 and γ_0 in Eq. (4) and Eq. (2) are adjusted accordingly.

The parameter α_tap as well as the start z_0 of the undulator tapering are scanned for maximum radiation power, as shown in Fig. 3. Optimum tapering is achieved for $\alpha_\mathrm{tap} = 2.52$ and $z_0 = 3.25 \cdot L_\mathrm{u} = 8.151\,\mathrm{m}$, meaning a tapering start within the fourth radiator module. The corresponding K values (orange curve in Fig. 2) are in good agreement with the ones found by the iterative method.

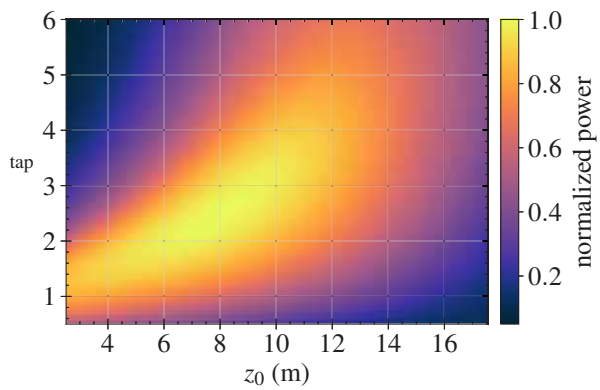

Figure 3: Radiation power (normalized) resulting from steady-state simulations of the radiator beamline with different tapering received from Eq. (2).

ISBN: 978-3-95450-227-1 ISSN: 2673-5490 doi:10.18429/JACoW-IPAC2022-TUPOPT023

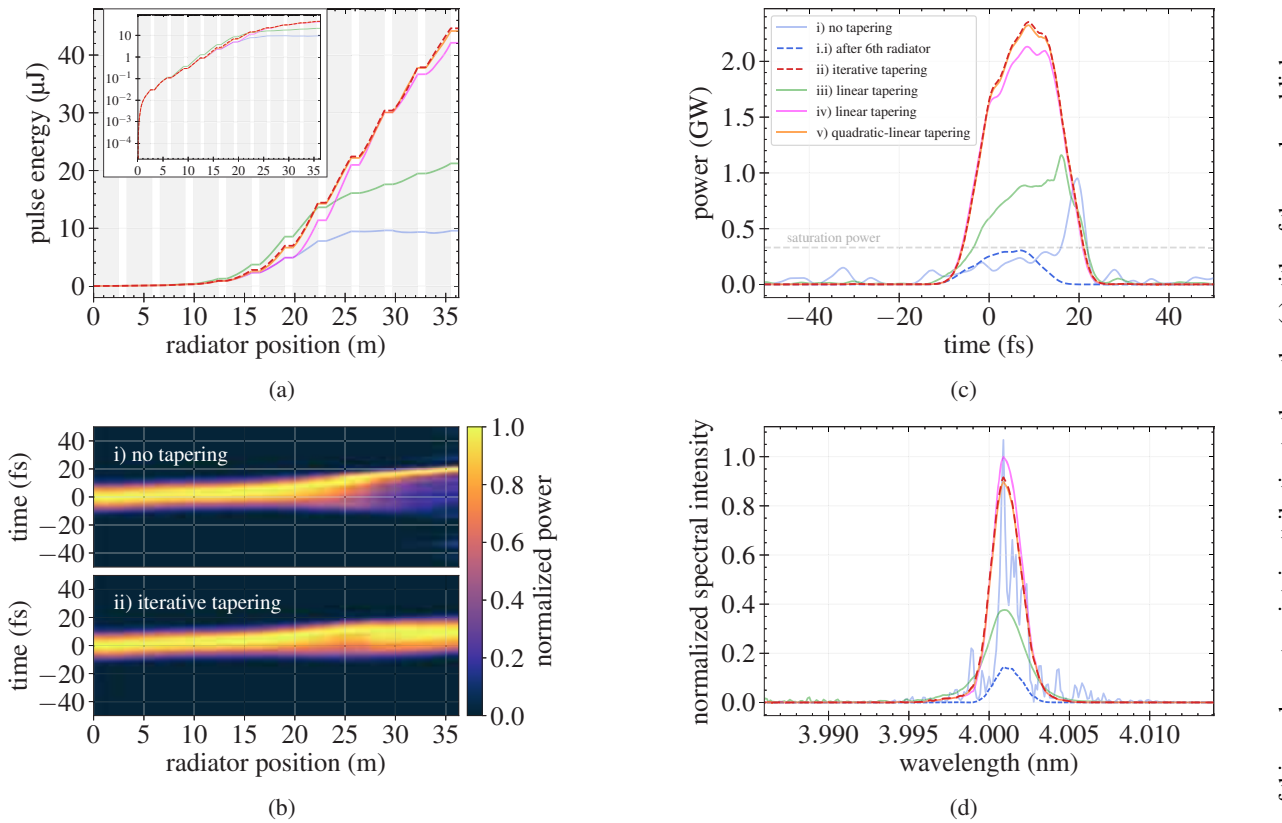

Figure 4: (a) Evolution of the pulse energy (in linear and logarithmic scale) and (b) normalized power profiles for different tapering methods along the radiator beamline. Radiator modules are indicated in gray. (c) Temporal and (d) spectral profiles of the FEL radiation at the exit of the radiator beamline for different tapering methods. The expected saturation power is indicated as a dashed gray line. For the not tapered case, the profiles close to saturation are also shown as dashed blue lines.

Results

Based on the presented optimum sets of K values, time-dependent simulations of the whole EEHG and FEL beamline are performed. Figure 4a shows the resulting energy in the radiation pulse along the radiator for each tapering method. The pulse energy is calculated by integrating the power from −20 fs to 25 fs. The evolution of the normalized power profiles along the beamline is illustrated in Fig. 4b. The corresponding power profiles as well as the spectra after the last radiator module are shown in Fig. 4c and 4d.

Following the 3D approximation given in [10, 11] yields a saturation power of $P_{\mathrm{sat}} \approx 0.33\,\mathrm{GW}$. Note that saturation is reached approximately within the 6th radiator module, and in the untapered case additional energy is extracted from the electrons due to an onwards slipping radiation pulse.

The highest peak power of about 2.3 GW is achieved for the iterative method and the quadratic-linear tapering (dashed red and orange curve). Here, the pulse energy is a factor of 4 larger than for the untapered case, a factor of 9 compared to the pulse energy close to saturation after the 6th radiator module. Already a linear tapering starting with the second module is sufficient to increase the pulse energy and to restore a Gaussian-like spectrum (green curve). Higher peak power and intensity can be achieved when initializing the linear tapering close to saturation (magenta curve). Note that this method also provides the highest peak intensity, but a smaller peak power and pulse energy than the iterative and quadratic-linear tapering methods. Analysis has shown that this is due to a different transverse field distribution, which is also affected by the undulator tapering.

CONCLUSION

Highest peak power is achieved by tapering each radiator module one by one iteratively. Similar results are obtained from quadratic-linear tapering based on a fit formula. Linear tapering showed comparable results when starting close to the saturation point. Results suggest that also the transverse field distribution should be taken into account when tapering.

ACKNOWLEDGMENTS

The authors gratefully acknowledge the Gauss Centre for Supercomputing e.V. (www.gauss-centre.eu) for funding this project by providing computing time on the GCS Supercomputer JUWELS [12] at Jülich Supercomputing Centre (JSC). This research was supported through the Maxwell computational resources operated at DESY, Hamburg. This work has been financially supported by BMBF within the project “05K2019-STAR”.

ISBN: 978-3-95450-227-1 ISSN: 2673-5490 doi:10.18429/JACoW-IPAC2022-TUPOPT023

REFERENCES

[1] G. Stupakov, "Using the Beam-Echo Effect for Generation of Short-Wavelength Radiation", *Phys. Rev. Lett.*, vol. 102, p. 074801, 2009. doi:10.1103/PhysRevLett.102.074801

[2] W. M. Fawley *et al.*, "Tapered undulators for SASE FELs", *Nucl. Instrum. Methods A*, vol. 483, pp. 537-541, 2002. doi:10.1016/S0168-9002(02)00377-7

[3] E. A. Schneidmiller and M. V. Yurkov, "Optimization of a high efficiency free electron laser amplifier", *Phys. Rev. ST Accel. Beams*, vol. 18, p. 030705, 2015. doi:10.1103/PhysRevSTAB.18.030705

[4] S. Reiche, "GENESIS 1.3: a fully 3D time-dependent FEL simulation code", *Nucl. Instrum. Methods A*, vol. 429, pp. 243-248, 1999. doi:10.1016/S0168-9002(99)00114-X

[5] S. Reiche, "Update on the FEL Code Genesis 1.3", in *Proc. 36th Int. Free Electron Laser Conf. (FEL'14)*, Basel, Switzerland, paper TUP019, pp. 403-407, Aug. 2014.

[6] L. Schaper *et al.*, "Flexible and Coherent Soft X-ray Pulses at High Repetition Rate: Current Research and Perspectives", *Applied Sciences*, vol. 11(20), p. 9729, 2021. doi:10.3390/app11209729

[7] W. Ackermann *et al.*, "Operation of a free-electron laser from the extreme ultraviolet to the water window", *Nature Photonics*, vol. 1, pp. 336-342, 2007. doi:10.1038/nphoton.2007.76

[8] S. Schreiber and B. Faatz, "The free-electron laser FLASH", *High Power Laser Science and Engineering*, vol. 3, p. e20, 2015. doi:10.1017/hpl.2015.16

[9] B. Faatz *et al.*, "Simultaneous operation of two soft x-ray free-electron lasers driven by one linear accelerator", *New Journal of Physics*, vol. 18, p. 062002, 2016. doi:10.1088/1367-2630/18/6/062002

[10] M. Xie, "Design optimization for an X-ray free electron laser driven by SLAC linac", *Proceedings Particle Accelerator Conference*, vol. 1, pp. 183-185, 1995. doi:10.1109/PAC.1995.504603

[11] M. Xie, "Exact and variational solutions of 3D eigenmodes in high gain FELs", *Nucl. Instrum. Meth. A*, vol. 445, pp. 59-66, 2000. doi:10.1016/S0168-9002(00)00114-5

[12] Damian Alvarez, Jülich Supercomputing Centre, "JUWELS Cluster and Booster: Exascale Pathfinder with Modular Supercomputing Architecture at Juelich Supercomputing Centre", *Journal of large-scale research facilities*, vol. 7, p. A138, 2021. doi:10.17815/jlsrf-7-183